Electronic Supplementary Material (ESI) for Journal of Materials Chemistry C.
This journal is © The Royal Society of Chemistry 2016

Electronic Supplementary Material (ESI) for Journal of Materials Chemistry C.
This journal is © The Royal Society of Chemistry 2015

Electronic Supplementary Information

Engineering the singlet-triplet energy splitting in a TADF molecule

Paloma L. Santos,*[a] Jonathan S. Ward,[b] Przemyslaw Data,[a] Andrei S. Batsanov,[b]
Martin R. Bryce,[b] Fernando B. Dias[a] and Andrew P. Monkman[a]

a- Physics Department, Durham University, South Road, Durham DH1 3LE, UK

b - Department of Chemistry, Durham University, South Road, Durham DH1 3LE, UK

Electronic Supplementary Material (ESI) for Journal of Materials Chemistry C.
This journal is © The Royal Society of Chemistry 2015

S1

Synthesis and characterization of (2,7-Bis(phenoxazin-10-yl)-9,9-dimethylthioxanthene-*S,S*-dioxide (DPO-TXO2)) and acceptor unit (9,9-dimethylxanthene-*S,S*-dioxide):

General experimental details

All reactions were carried out under an argon atmosphere unless otherwise stated. Starting materials were purchased commercially and were used as received. Solvents were dried using an Innovative Technology solvent purification system and were stored in ampoules under argon.

TLC analysis was carried out using Merck Silica gel 60 F_{254} TLC plates and spots were visualised using a TLC lamp emitting at 365, 312 or 254 nm. Silica gel column chromatography was performed using silica gel 60 purchased from Sigma Aldrich.

^{1}H and ^{13}C NMR spectroscopy was carried out on Bruker AV400, Varian VNMRS 500 and 700, and Varian Inova 500 NMR spectrometers. Residual solvent peaks were referenced as described in the literature, [1] and all NMR data was processed in MestReNova V10.

Melting points were carried out on a Stuart SMP40 machine with a ramping rate of 4 °C min^{-1}. Videos were replayed manually to accurately determine the melting point.

High resolution mass spectroscopy was carried out on a Waters LCT Premier XE using ASAP ionisation. Samples were analysed directly as solids using N_2 at 350 °C.

Elemental analysis was performed on an Exeter Analytical E-440 machine.

Any stated use of hexane refers to a mix isomers grade.

Synthesis and characterisation

- Synthesis of 9,9-dimethylthioxanthene

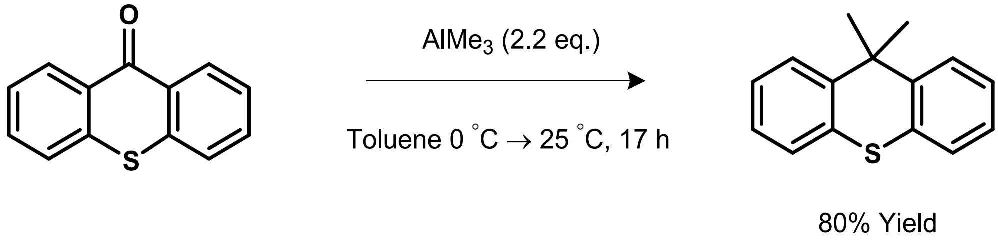

This procedure was followed exactly as reported in the literature, but scaled down by a factor of 12.5.[2]

- Synthesis of 2,7-dibromo-9,9-dimethylthioxanthene

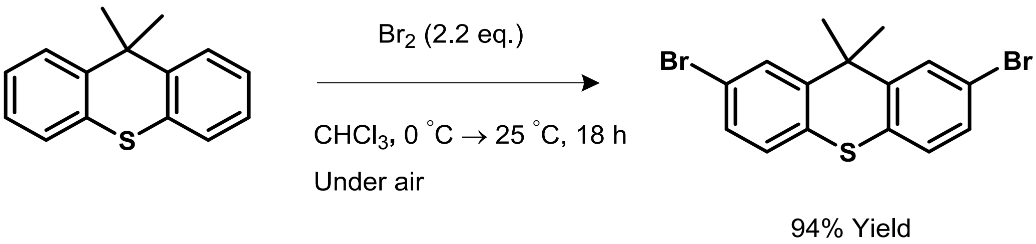

To a solution of 9,9-dimethylthioxanthene (4.60 g, 20.4 mmol, 1 eq.) in $CHCl_3$ (25 mL) was slowly added bromine (7.17 g/2.3 mL, 44.9 mmol, 2.2 eq.) at 0 °C with stirring. The reaction mixture was allowed to warm to ambient temperature and was stirred for a further 18 h. The reaction mixture was transferred to a separating funnel and sodium thiosulfate solution (10 mL) was added. The organic layer was separated and the aqueous layer was extracted with CH_2Cl_2 (3 × 20 mL). The combined organic layers were washed with water (30 mL) and brine (30 mL), and was then dried with $MgSO_4$ and filtered. Removal of solvent under reduced pressure gave pure product as a brown crystalline solid (7.35 g, 94% yield).

^{1}H NMR (400 MHz, $CDCl_3$) δ 7.62 (d, *J* = 2.0 Hz, 2H), 7.33 (dd, *J* = 8.2, 2.0 Hz, 2H), 7.28 (d, *J* = 8.2 Hz, 2H), 1.64 (s, 6H); ^{13}C NMR (101 MHz, $CDCl_3$) δ 143.9, 131.8, 129.3, 128.7, 128.2, 120.9, 40.7, 24.9; HRMS-ASAP$^+$ *m/z* calculated for $C_{15}H_{13}SBr_2$ $[M+H]^+$

382.9105, found: 382.9104; Anal. Calc. for $C_{15}H_{12}SBr_2$ C, 46.90; H, 3.15; N: 0.00. Found: C, 46.91; H, 3.16; N, 0.00; m.p. 117 – 119 °C

- Synthesis of 2,7-dibromo-9,9-dimethylthioxanthene-*S,S*-dioxide

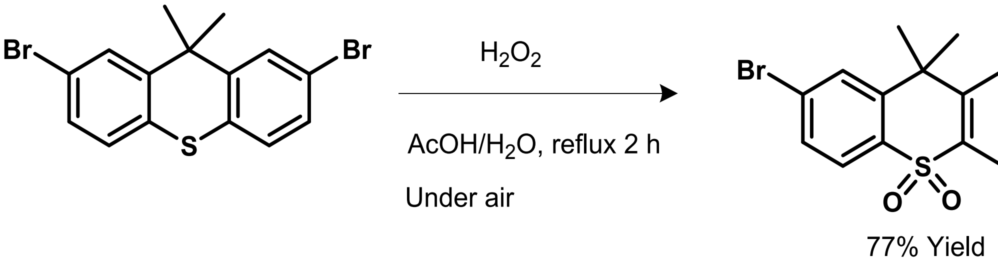

To a stirring solution of 2,7-dibromo-9,9-dimethylthioxanthene (3.50 g, 9.11 mmol, 1 eq.) in AcOH (150 mL) at 80 °C was slowly added H_2O_2 (40 ml, 35% wt in H_2O) *via* a reflux condenser. The reaction mixture was refluxed for 2 h and was then left to cool to room temperature which resulted in the precipitation of pure product which was collected by filtration and was washed with water. Further product can be precipitated by addition of more H_2O to the filtrate. The product was dried at 70 °C overnight to obtain pure product as a white solid (2.90 g, 76% yield)

^{1}H NMR (400 MHz, DMSO-d_6) δ 8.15 (d, *J* = 1.8 Hz, 2H), 8.01 (d, *J* = 8.3 Hz, 2H), 7.86 (dd, *J* = 8.3, 1.8 Hz, 2H), 1.83 (s, 6H); ^{13}C NMR (101 MHz, DMSO-*d*$_6$) δ 147.2, 134.8, 131.3, 129.9, 127.7, 125.4, 39.4, 29.9.; HRMS-ASAP$^+$ *m/z* calculated for $C_{15}H_{13}SBr_2O_2$ [M+H]$^+$ 414.9003, found: 414.8990; Anal. Calc. for $C_{15}H_{12}SBr_2O_2$ C, 43.30; H, 2.91; N, 0.00. Found: C, 43.37; H, 2.87; N, 0.00; m.p. 157 – 159 °C

- Synthesis of 9,9-dimethylthioxanthene-*S,S*-dioxide

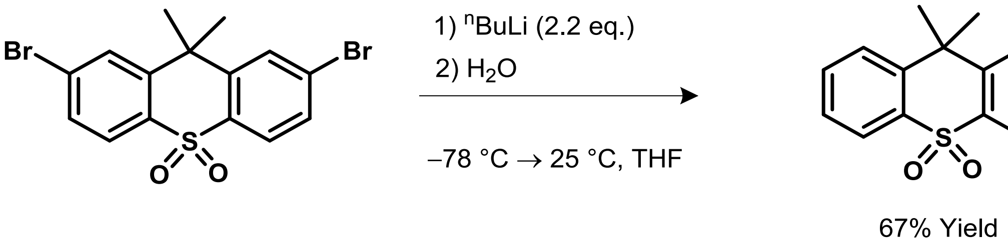

To a solution of 2,7-dibromo-9,9-dimethylthioxanthene-*S,S*-dioxide (235 mg, 565 μmol, 1 eq.) in THF (10 mL) under argon at −78 °C was added dropwise ^{n}BuLi (2.5 M in hexane, 0.50 mL, 1.24 mmol, 2.2 eq.). The solution was stirred at −78 °C for one hour. Water (50 mg, 2.83 mmol, 5 eq.) was added slowly to the reaction and it was allowed to warm to room temperature. Water (15 mL) was added to the reaction mixture and the aqueous layer was extracted with CH_2Cl_2 (3 × 50 mL). The combined organic extracts were dried with $MgSO_4$ and filtered. Removal of solvent under reduced pressure gave a white residue. The residue was purified further by silica gel column chromatography by directly loading on to the column in CH_2Cl_2 (1 mL). The product was eluted by gradient elution from 80:20 *v/v* CH_2Cl_2: Hexane, moving to 100% CH_2Cl_2. Removal of solvent under reduced pressure gave pure compound as a white solid (98 mg, 67% yield).

^{1}H NMR (400 MHz, DMSO-d_6) δ 8.08 (dd, *J* = 7.8, 1.5 Hz, 2H), 7.97 (dd, *J* = 8.1, 1.1 Hz, 2H), 7.74 (m, 2H), 7.63 (m, 2H), 1.82 (s, 6H); ^{13}C NMR (101 MHz, DMSO-d_6) δ 145.4, 135.9, 133.4, 127.9, 126.7, 123.3, 38.9, 30.4; HRMS-ASAP$^+$ *m/z* calculated for $C_{15}H_{15}SO_2$ [M+H]$^+$ 259.0793, found: 259.0803; Anal. Calc. for $C_{15}H_{14}SO_2$ with 0.8% wt. CH_2Cl_2 C, 69.30; H, 5.43; N, 0.00. Found: C, 69.05; H, 5.45; N, 0.01; m.p. 161 – 163 °C.

- Synthesis of 2,7-Bis(phenoxazin-10-yl)-9,9-dimethylthioxanthene-*S,S*-dioxide (DPO-TXO2)

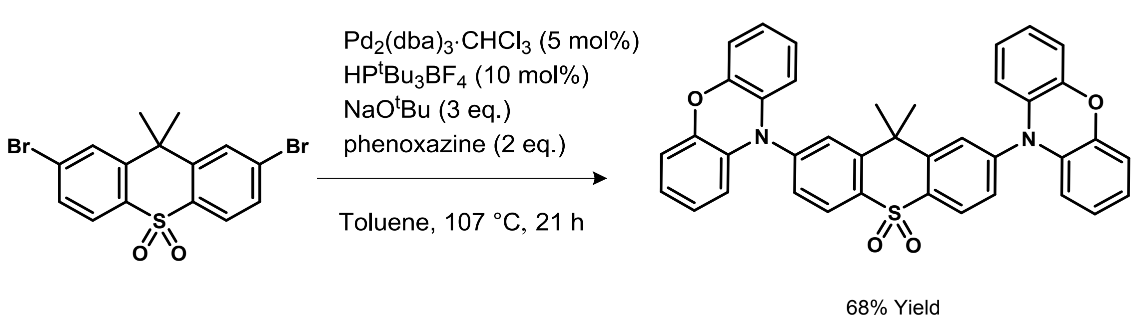

This compound was synthesised using a modified literature procedure for 2,8-Bis[*N,N*-di(4-butylphenyl)amino]dibenzothiophene-*S,S*-dioxide.[3]

2,7-dibromo-9,9-dimethylthioxanthene-*S,S*-dioxide (400 mg, 0.961 mmol, 1 eq.) and phenoxazine (352 mg, 1.92 mmol, 2 eq.) were dried under vacuum for 30 minutes in a two-neck 100 mL round-bottomed flask fitted with a reflux condenser. The flask was back-filled with argon and dry toluene (20 mL) was added. The reaction mixture was bubbled with argon for 30 minutes, then $Pd_2(dba)_3 \cdot CHCl_3$ (49 mg, 47 µmol, 0.05 eq.) and $HP^tBu_3BF_4$ (28 mg, 96 µmol, 0.1 eq.) was added and the reaction mixture was bubbled with argon for a further 30 minutes. NaO^tBu (277 mg, 2.88 mmol, 3 eq.) was added under a high flow of argon and the reaction was then heated to 107 °C with stirring for 21 h. At the end of the reaction the solvent was removed under reduced pressure and the crude mixture was purified by silica gel column chromatography eluting with 80% CH_2Cl_2/hexane. Removal of solvent under reduced pressure gave the product as a yellow solid. (404 mg, 68% yield). The title compound can be sublimed under vacuum (1×10^{-1} mbar, > 350 °C). Crystals suitable for X-ray diffraction were obtained by slow evaporation from 1:1 *v/v* 2-methylTHF:CH_2Cl_2.

^1H NMR (400 MHz, CD_2Cl_2) δ 8.43 (d, *J* = 8.2 Hz, 2H), 7.80 (d, *J* = 1.9 Hz, 2H), 7.59 (dd, *J* = 8.2, 1.9 Hz, 2H), 6.76 – 6.67 (m, 8H), 6.66 – 6.60 (m, 4H), 5.98 (d, *J* = 1.4, 2H), 5.96 (d, *J* = 1.4 Hz, 2H), 1.89 (s, 6H); ^{13}C NMR (176 MHz, CD_2Cl_2) δ 149.7, 144.4, 144.0, 137.0, 134.0, 130.8, 129.1, 127.8, 123.8, 122.5, 116.1, 113.8, 40.3, 31.0; HRMS-ASAP$^+$ *m/z* calculated for $C_{39}H_{28}N_2O_4S$ $[M]^+$ 620.1770, found: 620.1791; Anal. Calc. for $C_{39}H_{28}N_2O_4S$ C, 75.47; H, 4.55; N, 4.51. Found: C, 75.51; H, 4.56; N, 4.48, m.p. 348 – 350 °C.

^1H and ^{13}C NMR spectra of new compounds

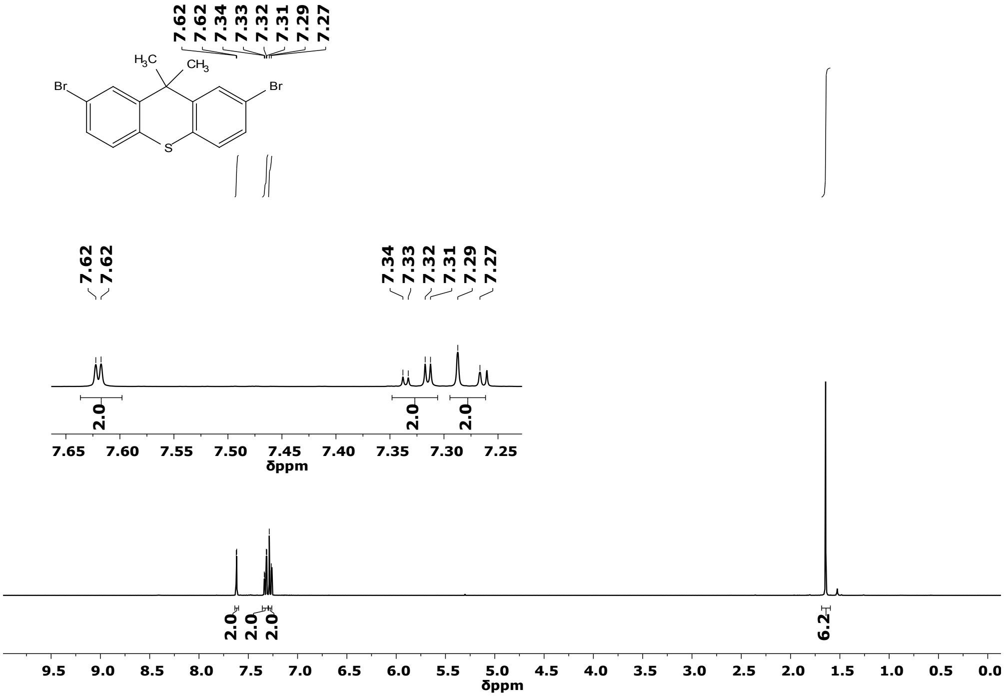

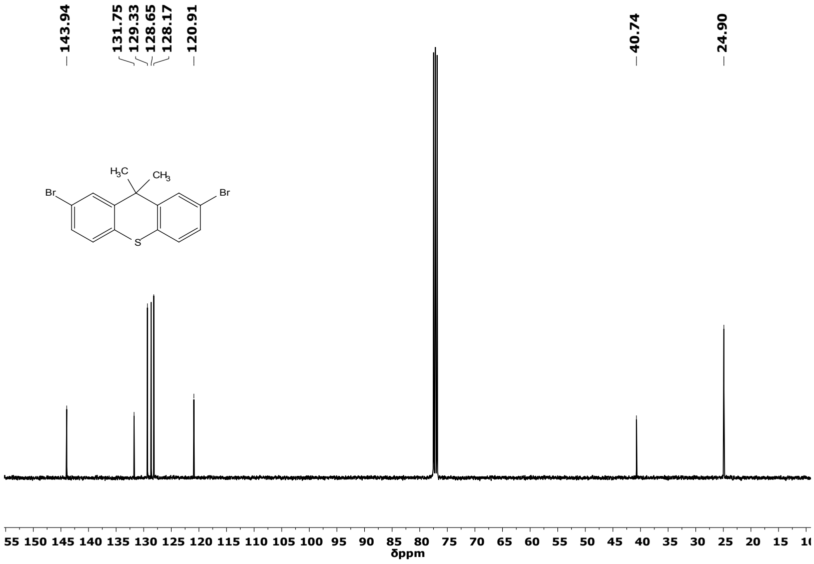
143.94
131.75
129.33
128.65
128.17
120.91
40.74
24.90
H_3C
CH_3
Br
Br
S
55 150 145 140 135 130 125 120 115 110 105 100 95 90 85 80 75 70 65 60 55 50 45 40 35 30 25 20 15 1
δppm

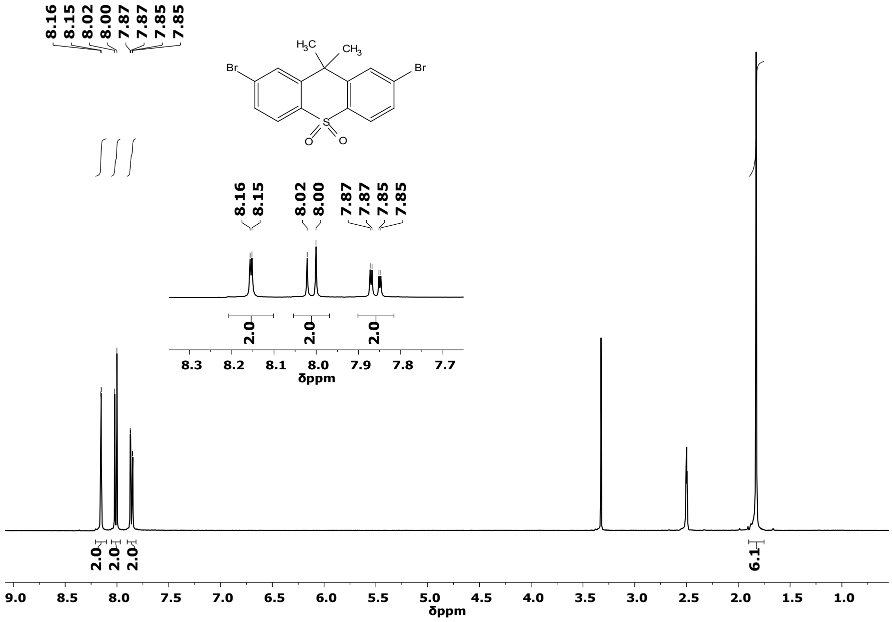
8.16
8.15
8.02
8.00
7.87
7.87
7.85
7.85
H_3C
CH_3
Br
Br
S
O
O
2.0
2.0
2.0
8.3 8.2 8.1 8.0 7.9 7.8 7.7
δppm
2.0
2.0
2.0
6.1
9.0 8.5 8.0 7.5 7.0 6.5 6.0 5.5 5.0 4.5 4.0 3.5 3.0 2.5 2.0 1.5 1.0
δppm

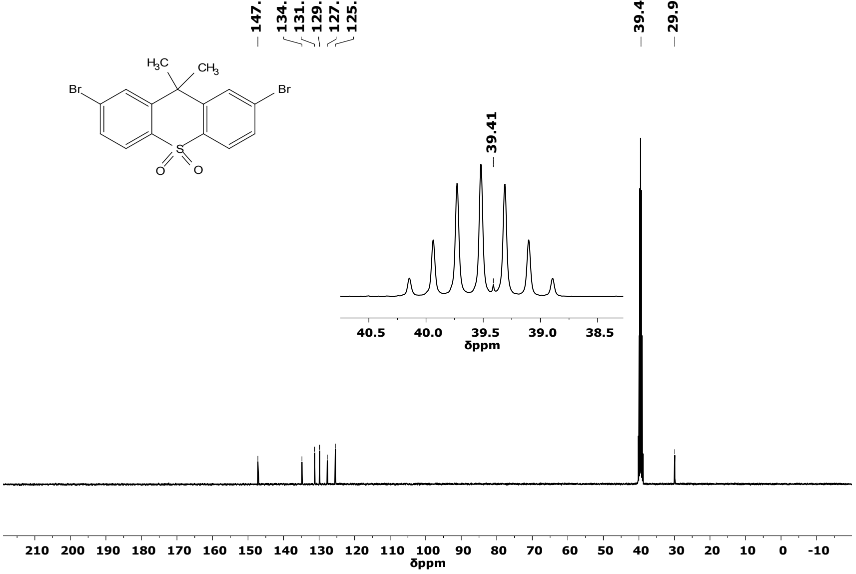
147.23
134.83
131.27
129.86
127.69
125.42
39.41
29.90
H_3C
CH_3
Br
Br
S
O
O
39.41
40.5 40.0 39.5 39.0 38.5
δppm
210 200 190 180 170 160 150 140 130 120 110 100 90 80 70 60 50 40 30 20 10 0 -10
δppm

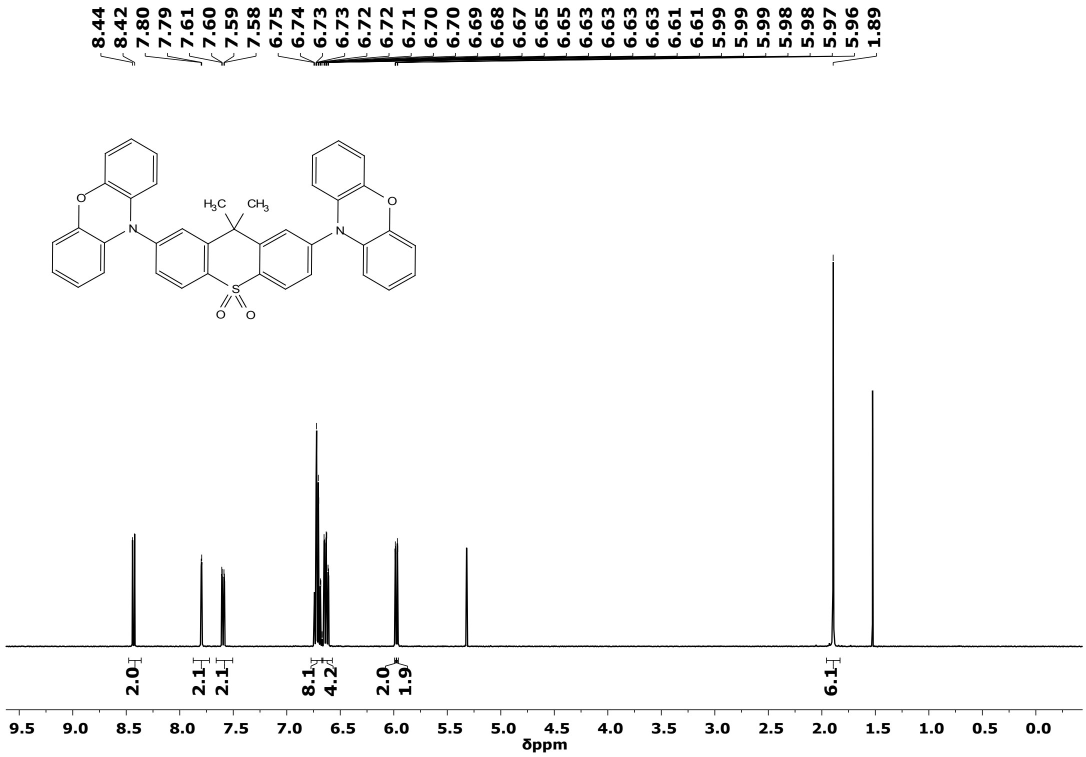

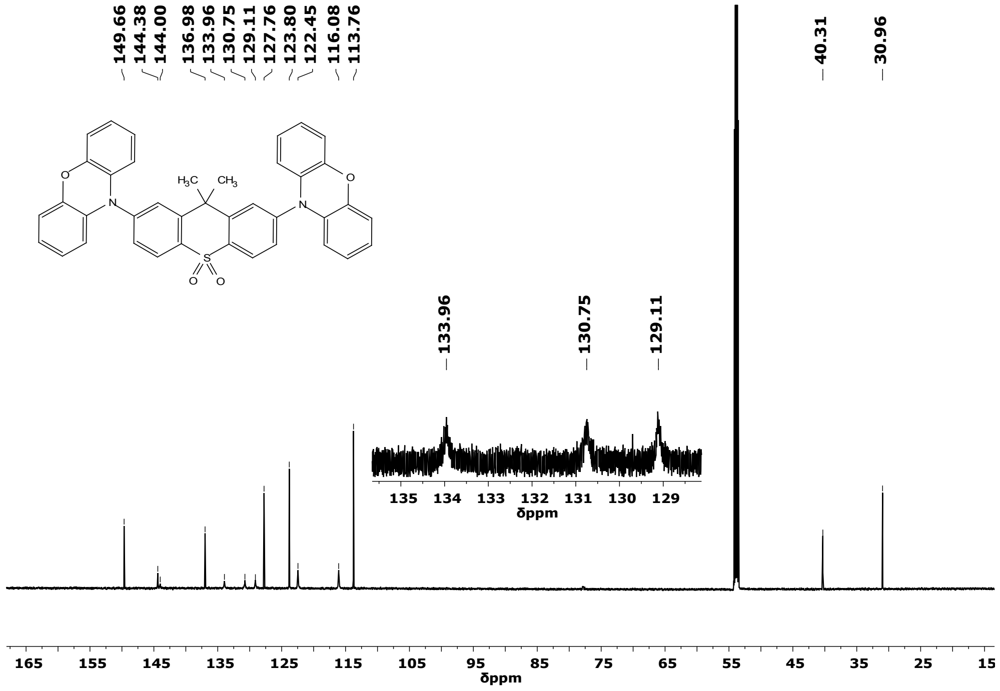

S2

From the potentials of the onset of these redox peaks it is possible to estimate the ionization potential (IP) and the electron affinity (EA) provided that these potentials are expressed on the absolute potential scale i.e. with respect to the vacuum level. The absolute potential of Fc/Fc$^+$ in nonaqueous electrolytes is 5.1 V.[4–6] This leads to the following equation:

$$IP(eV) = |e|(E_{ox(onset)} + 5.1) \qquad (1)$$

$$EA(eV) = -|e|(E_{red(onset)} + 5.1) \qquad (2)$$

The HOMO-LUMO levels were determined electrochemically, using cyclic voltammetry (CV) analysis by the estimation of the electron affinity and the ionization potentials which are similar to the HOMO and LUMO energies. [6,7] The results are shown in figure S2.

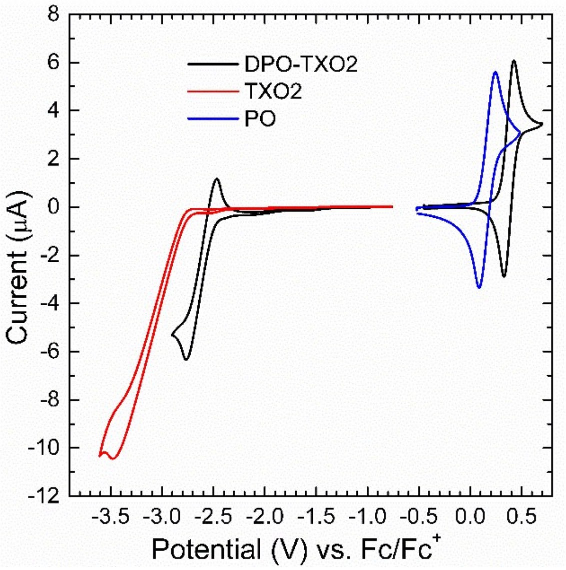

Figure S2 Cyclic voltammetry (CV) analysis by the estimation of the electron affinity and the ionization potentials for DPO-TXO2 (black), TXO2 acceptor unit (red) and Phenoxazine (PO) (blue).

Compound	**HOMO (eV)**	**LUMO (eV)**
DPO-TXO2	**-5.37**	**-2.61**
Phenoxazine	**-5.15**	**-**
TXO2	**-**	**-2.33**

Materials and methods

The electrochemical cell comprised of platinum electrode with a 1 mm diameter of working area as a working electrode, an Ag/AgCl electrode as a reference electrode and a platinum coil as an auxiliary electrode. Cyclic voltammetry measurements were conducted at room temperature at a potential rate of 50 mV/s and were calibrated against a ferrocene/ferrocenium redox couple.

The molecules investigated have a wide HOMO-LUMO gap which necessitated the use of different solvents: THF for reduction down to -3.5 V and DCM for oxidation up to +2.0 V.

All solvents for synthesis were dried before use. Other commercially available substances and reagents were used without purification. Electrochemical measurements were conducted in 1.0 mM concentrations of all compounds for all cyclic voltammetry measurements. Electrochemical studies were undertaken in 0.1 M solutions of Bu_4NBF_4, 99% (Sigma Aldrich) in dichloromethane (DCM) or THF solvent, CHROMASOLV®, 99.9% (Sigma Aldrich) at room temperature.

S3

Figure S3 shows the charge transfer (CT) steady state spectra of DPO-TXO2 diluted in MCH. The spectra present just the CT emission and not the acceptor or donor localized emissions excited at different wavelengths. The CT emission is identified when DPO-TXO2 is excited at 313 nm (peak absorption of the donor), at 268 nm (peak absorption of the acceptor) and at 380 nm (peak absorption observed just in the D-A-D molecule, not in the individual units). All the spectra were normalized considering the intensity of emitted light (I_f), equation 3, [8]

$$I_f = \emptyset_F \, I_0(1 - 10^{-OD}) \tag{3}$$

where $\emptyset_F$ is the quantum efficiency, I_0 is the incident radiant power and OD the optical density. As can be seen, the CT state shows the highest intensity when donor unit is excited, being the most efficient way to create the CT state. Inset graph shows these normalized spectra. When DPO-TXO2 is excited at 268 nm, the emission is slight blue shifted, due to the contribution of the acceptor emission localized in higher energy (^1LE_A).

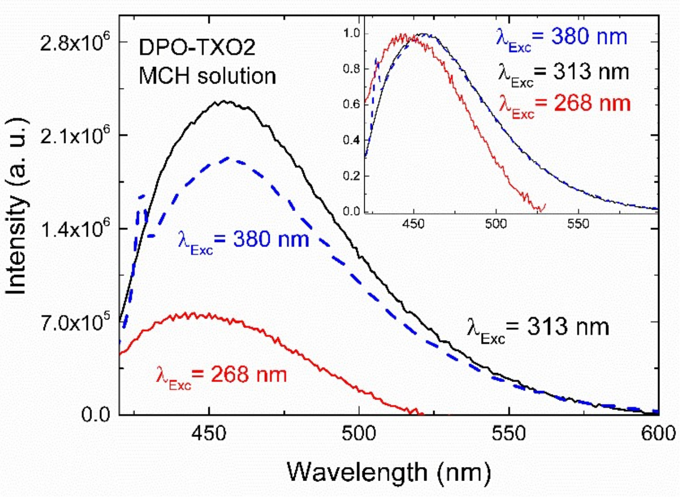

Figure S3 Photoluminescence spectra (PL) of DPO-TXO2 excited at different wavelengths (268 nm, 313 nm and 380 nm). Inset graph shows these spectra normalized.

S4

Figure S4 shows the comparison between degassed solution (black line) and non-degassed (red line), steady state spectra of DPO-TXO2 in MCH solution. Upon removing the oxygen, the intensity decreases by a factor of 3.10. Inset graph show the normalized spectra.

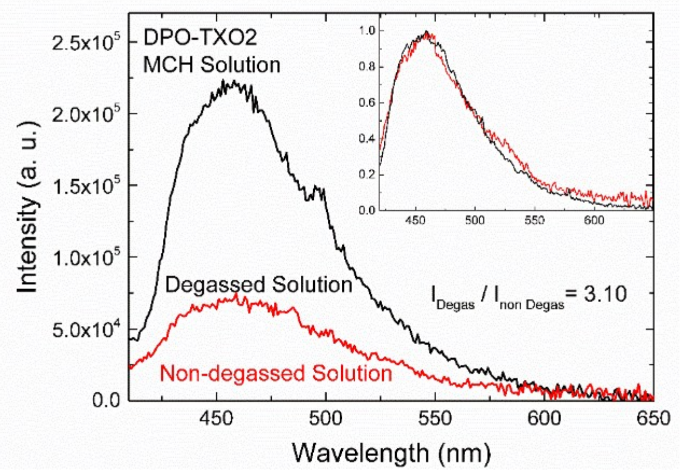

Figure S4 Photoluminescence spectra (PL) of DPO-TXO2 in degased and non-degassed MCH solutions. Inset graph shows these spectra normalized.

Equation 4 provides the emission contribution of TADF ($\bar{n}$), being unlikely to occur when the energy splitting between singlet and triplet states is larger than 0.1 eV. [9,10]

$$\bar{n} = \frac{I_{degas}}{I_{non\ degas}} - 1 = \int \frac{I_{TADF\ (t)dt}}{I_{PF\ (t)dt}} \tag{4}$$

Therefore, DPO-TXO2 has $\bar{n}$ = 2.10 in MCH solution.

S5

Figure S5 shows the comparison between degassed solution (black line) and non degassed (red line), steady state spectra of DPO-TXO2 in toluene solution. Upon removing the oxygen, the intensity decreases by a factor of 5.80. Inset graph show the normalized spectra. Therefore, DPO-TXO2 has $\bar{n}$ = 4.80 in toluene solution.

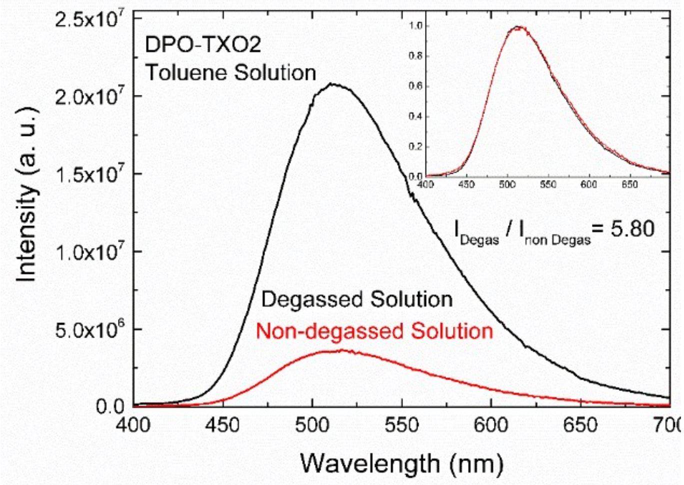

Figure S5 Photoluminescence spectra (PL) of DPO-TXO2 in degased and non-degassed toluene solutions. Inset graph shows these spectra normalized.

S6

Figure S6 shows the delayed fluorescence spectra of DPO-TXO2 at different laser excitation doses. The spectra were collected with time delay of 100 ns (region A, figure 6a in the manuscript). Inset graph shows the area of each spectrum as a function of excitation dose, and a linear gradient was found (1.045 ± 0.005) confirming the thermally assisted mechanism.

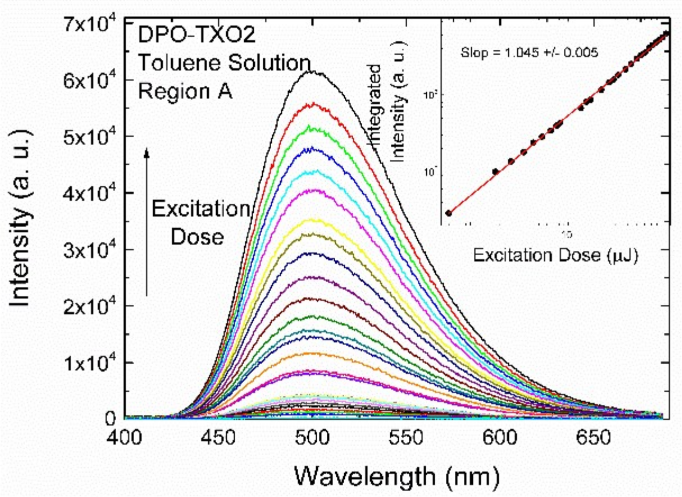

Figure S6 Delayed fluorescence spectra of DPO-TXO2 in different laser excitation doses. Inset graph shows the area of each spectrum as a function of excitation dose. Spectra collected with TD = 100 ns.

S7

Figure S7 shows the delayed fluorescence spectra of DPO-TXO2 in different laser excitation doses. The spectra were collected with time delay located of 10µs (region B, figure 6.a in the manuscript). Inset graph shows the area of each spectrum as a function of excitation dose, and a linear gradient was found (1.025 ± 0.004) confirming the thermally assisted mechanism.

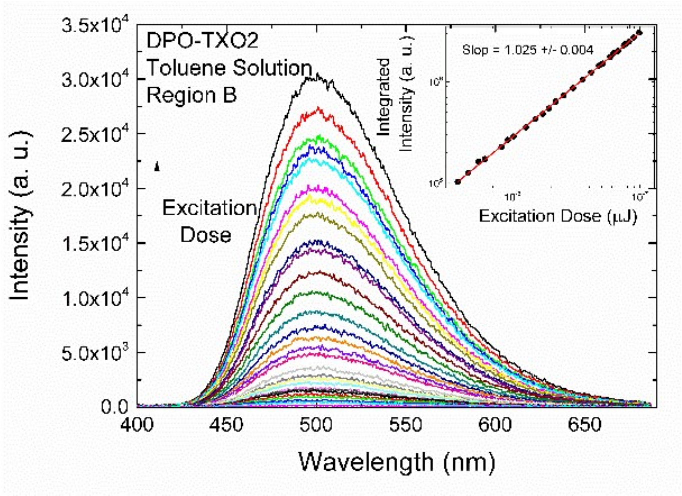

Figure S7 Delayed fluorescence spectra of DPO-TXO2 in different laser excitation doses. Inset graph shows the area of each spectrum as a function of excitation dose. Spectra collected with TD = 10 μs.

S8

Figure S8 shows the Current density *versus* Bias and Brightness *versus* Bias for DPO-TXO2:CBP (blue) and DPO-TXO2:DPEPO (red) devices. The turn on voltage of the device in DPEPO host is lower than the device in CBP, showing a better performance for DPEPO device. The maximum brightness levels of the DPEPO device are higher, showing again that DPEPO is the most appropriate host for DPO-TXO2.

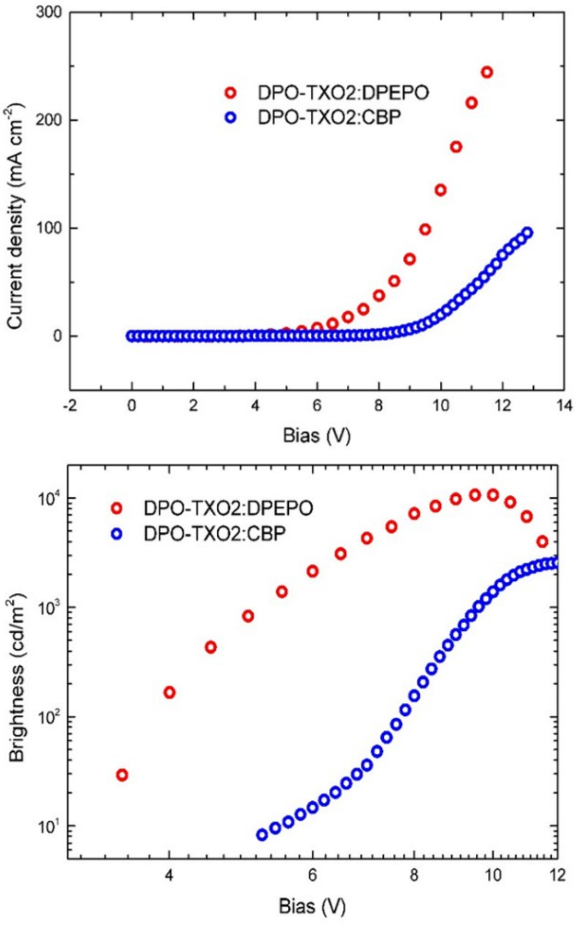

Figure S8 Current density *versus* Bias and Brightness *versus* Bias for DPO-TXO2:DPEPO and DPO-TXO2:CBP devices.

References

1 G. R. Fulmer, A. J. M. Miller, N. H. Sherden, H. E. Gottlieb, A. Nudelman, B. M. Stoltz, J. E. Bercaw and K. I. Goldberg, *Organometallics*, 2010, **29**, 2176–2179.

2 D. J. H. Emslie, J. M. Blackwell, J. F. Britten and L. E. Harrington, *Organometallics*, 2006, **25**, 2412–2414.

3 F. B. Dias, K. N. Bourdakos, V. Jankus, K. C. Moss, K. T. Kamtekar, V. Bhalla, J. Santos, M. R. Bryce and A. P. Monkman, *Adv. Mater.*, 2013, **25**, 3707–3714.

4 R. Rybakiewicz, P. Gawrys, D. Tsikritzis, K. Emmanouil, S. Kennou, M. Zagorska and A. Pron, *Electrochim. Acta*, 2013, **96**, 13–17.

5 S. Trasatti, *Pure Appl. Chem.*, 1986, **58**, 955–966.

6 P. Data, R. Motyka, M. Lapkowski, J. Suwinski and A. P. Monkman, *J. Phys. Chem. C*, 2015, **119**, 20188–20200.

7 J.-L. Bredas, *Mater. Horiz.*, 2014, **1**, 17–19.

8 G. G. Guilbault, *Practical Fluorescence - Second edition,* **3**, 1990.

9 C. Baleizão and M. N. Berberan-Santos, *J. Chem. Phys.*, 2007, **126**, 1–8.

10 F. B. Dias, *R. Soc.*, 2015, **373**, 20140447.